Supplementary Information for: "On the scale dependence in the dynamics of rupture: constant fracture energy versus size-dependent breakdown work"

Federica Paglialunga[a,1], François Passelègue[a], Nicolas Brantut[b], Fabian Barras[c], Mathias Lebihain[a], Marie Violay[a]

[a] *Laboratoire de Mécanique des Roches, École Polytechnique Fédérale de Lausanne, Switzerland*
[b] *Department of Earth Sciences, University College London, London, UK*
[c] *NJORD Centre for Studies of the Physics of the Earth, University of Oslo, Norway*

SI 1. Fracture energy inversion through LEFM

In LEFM framework, the stress perturbation around the crack tip was computed as a function of the distance from the crack tip itself for given values through:

$$\Delta\tau(\theta, r, C_{\mathrm{f}}) = \frac{K_{\mathrm{II}}(C_{\mathrm{f}})}{\sqrt{2\pi}}\Sigma^{\mathrm{II}}_{\mathrm{xy}}(\theta, C_{\mathrm{f}}) \tag{1}$$

where (θ, r) are polar coordinates with origin at the crack tip, $K_{\mathrm{II}}(C_{\mathrm{f}})$ the mode II stress intensity factor and $\Sigma^{\mathrm{II}}_{\mathrm{xy}}(\theta, C_{\mathrm{f}})$ the angular variation. The stress intensity factor was related to the fracture energy assuming an equilibrium with the energy release rate following:

$$G_{\mathrm{II}} = \frac{(1-\nu^2)}{E}K^2_{\mathrm{II}}(C_{\mathrm{f}})f_{\mathrm{II}}(C_{\mathrm{f}}) \tag{2}$$

where $f_{\mathrm{II}}(C_{\mathrm{f}})$ is a function of the rupture velocity. From the last relation $K_{\mathrm{II}}(C_{\mathrm{f}})$ could be written as a function of the fracture energy and rupture velocity only. Since the system was initially loaded (macroscopic loads), the stress distribution at the crack tip was given by initial $(\sigma_{\mathrm{x}}, \sigma_{\mathrm{y}})$ and residual (τ) stresses and the respective singular contributions of the stress field $(\Delta\sigma_{\mathrm{x}}, \Delta\sigma_{\mathrm{y}}, \Delta\tau)$. Considering this, to compare the experimental measurements to LEFM theoretical predictions, the initial strain was subtracted from $\varepsilon_{\mathrm{xx}}, \varepsilon_{\mathrm{yy}}$ and the residual

Email address: federica.paglialunga@epfl.ch (Federica Paglialunga)

strain from ε_{xy} to obtain strain variations resulting from the rupture propagation ($\Delta\varepsilon_{xx}, \Delta\varepsilon_{yy}, \Delta\varepsilon_{xy}$). By following the procedure described in Svetlizky and Fineberg (2014), the fracture energy was inverted from the strain increase assuming our local estimates of rupture velocity.

SI 2. Fracture energy inversion through CZM

The procedure to compute the shear stress change field around the crack tip through the cohesive zone model followed the solutions already derived in Poliakov et al. (2002) and Kammer and McLaskey (2019). Complex variables need to be defined as:

$$\begin{aligned} z_{\mathrm{d}} &= x + i\alpha_{\mathrm{d}} y; \\ z_{\mathrm{s}} &= x + i\alpha_{\mathrm{s}} y \end{aligned} \tag{3}$$

with $\alpha_d = \sqrt{1 - C_{\mathrm{f}}^2/C_{\mathrm{p}}^2}$, $\alpha_{\mathrm{s}} = \sqrt{1 - C_{\mathrm{f}}^2/C_{\mathrm{s}}^2}$. For a cohesive linear cohesive zone we can define the following analytic functions

$$\begin{aligned} M_d &= \frac{\tau_{\mathrm{p}} - \tau_{\mathrm{r}}}{\pi} \left[\left(1 + \frac{z_{\mathrm{d}}}{x_{\mathrm{c}}}\right) \arctan\left(\frac{z_{\mathrm{d}}}{x_{\mathrm{c}}}\right)^{-0.5} - \left(\frac{z_{\mathrm{d}}}{x_{\mathrm{c}}}\right)^{0.5} \right]; \\ M_s &= \frac{\tau_{\mathrm{p}} - \tau_{\mathrm{r}}}{\pi} \left[\left(1 + \frac{z_{\mathrm{s}}}{x_{\mathrm{c}}}\right) \arctan\left(\frac{z_{\mathrm{s}}}{x_{\mathrm{c}}}\right)^{-0.5} - \left(\frac{z_{\mathrm{s}}}{x_{\mathrm{c}}}\right)^{0.5} \right] \end{aligned} \tag{4}$$

The shear stress change can then be described as

$$\Delta\sigma_{xy}(x, y) = Re\left[4\alpha_{\mathrm{s}}\alpha_d M_d - (1 + \alpha_{\mathrm{s}}^2)^2 M_{\mathrm{s}}\right]/D \tag{5}$$

with $D(C_{\mathrm{f}}) = 4\alpha_{\mathrm{s}}\alpha_{\mathrm{d}} - (1 + \alpha_{\mathrm{s}}^2)^2$ the Rayleigh function.

SI 3. Numerical simulations

The illustrative numerical simulations were carried out through spectral boundary integral method (Morrissey and Geubelle, 1997). Mode III ruptures governed by the two-stage law were studied:

$$\tau_{\mathrm{f}}(D) = \begin{cases} \tau_{\mathrm{p}} - (\tau_{\mathrm{p}} - \tau_{\mathrm{mid}})D/D_{\mathrm{c,tip}}) & \text{if } D \leq D_{\mathrm{c,tip}}, \\ \tau_{\mathrm{mid}}(1 - (D - D_{\mathrm{c,tip}})/(D_{\mathrm{c,tip}} - D_{\mathrm{c,tail}})) & \text{if } D_{\mathrm{c,tip}} < D \leq D_{\mathrm{c,tail}}, \\ 0 & \text{else.} \end{cases} \tag{6}$$

where $\tau_{\mathrm{f}}(D)$ is the frictional stress acting along the interface, τ_0 the peak stress, τ_{mid} the stress at which the constitutive law transitions from the first stage weakening into the long-tailed weakening, $D_{\mathrm{c,tip}}$ the critical slip distance related to the first stage weakening and $D_{\mathrm{c,tail}}$ the critical slip distance related to the long-tailed weakening. The elastodynamic equilibrium relating shear stress τ to the ongoing slip rate V is given by

$$\tau(x,t) = \tau_{\mathrm{b}}(x,t) + \phi(x,t) - \mu V(x,t)/2C_{\mathrm{s}}, \tag{7}$$

where τ_{b} is the background stress on the fault, μ is the shear modulus of the surrounding material, and C_{s} is the shear wave speed. The term ϕ corresponds to the static and dynamic non-local stress redistribution due to slip. To study the influence of the dual-scale weakening, we compared numerical results given by two different constitutive relations. The first one is the standard slip weakening law while the second one presents a second weakening, occurring after $D_{\mathrm{c,tip}}$ is overcome, which releases stress for a much longer displacement. The second weakening distance was chosen by extrapolating from the experimental curves the slope of the second weakening and inferring from this the displacement corresponding to a total stress drop. For this reason the second weakening distance ($D_{\mathrm{c,tail}}$) was chosen to be $50 \cdot D_{\mathrm{c,tip}}$.

SI 4. Transition between scenario S1 and S2: critical background stress

It was shown in our simulations how different levels of background stress lead to different rupture dynamics. The critical background stress describing the transition between the two scenarios can be obtained by looking at dynamic fracture mechanics. Form Freund's approximation (Freund, 1998), the rupture velocity is proportional to G/G_{c} in the following way:

$$C_{\mathrm{f}} \propto G/G_{\mathrm{c}} = \frac{(\tau_{\mathrm{b}} - \tau_{\mathrm{r}})^2 \pi L}{2\mu D_{\mathrm{c}}(\tau_{\mathrm{p}} - \tau_{\mathrm{r}})\alpha_{\mathrm{s}}}. \tag{8}$$

For a fixed background stress τ_{b} and any rupture size L, a rupture driven by the second weakening mechanism is expected to propagate faster than a rupture

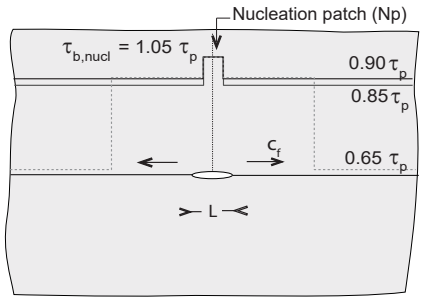

Figure 1: Scheme of the numerical setup with the initial background stress along the fault ($\tau_{\rm b}$), for both scenarios S1 (in solid black), S2 (in solid gray) and for the case with stress barrier (in dashed gray). An elevated stress patch $\tau_{\rm b,nucl}$ 5% above τ_0, in a small region at the center of the modeled fault (N_P), allows rupture nucleation.

driven by the first weakening mechanism if:

$$C_{\rm f,2} > C_{\rm f,1}, \frac{(\tau_{\rm b} - \tau_{\rm r,2})^2}{D_{\rm c,2}(\tau_{\rm p,2} - \tau_{\rm r,2})} > \frac{(\tau_{\rm b} - \tau_{\rm r,1})^2}{D_{\rm c,1}(\tau_{\rm p,1} - \tau_{\rm r,1})} \tag{9}$$

From this relation, one can then define a critical background stress $\tau_{\rm b}^*$ below which, the second weakening mechanism will control rupture dynamics:

$$\tau_{\rm b}^* = \frac{\eta\tau_{\rm r,1} - \tau_{\rm r,2}}{\eta - 1} \tag{10}$$

with $\eta = \sqrt{G_{\rm c,2}/G_{\rm c,1}}$. The critical value of background stress associated to our simulations is found to be $\tau_{\rm b}^* = 0.86$, value which well reflects the transition observed between S1 ans S2.

SI 5. Estimate of the fracture energy from natural earthquakes

The breakdown work of natural earthquakes has been estimated from values of seismic moment (M_0), source radius (r), static stress drop ($\Delta\sigma$) and radiated energy (E_r). The average slip ($\bar{D}$) was calculated for each events from the definition of the seismic moment which implies that (Aki, 1966)

$$\bar{D} = \frac{M_0}{\mu A} \tag{11}$$

where $A = \pi r^2$ is the rupture area. The breakdown work was then estimated from the relation described by Abercrombie and Rice (2005)

$$W_b = (\Delta\sigma - \sigma_a)\frac{\bar{D}}{2} \tag{12}$$

where σ_a is estimated following Beeler and Hickman (2004)

$$\sigma_a = \mu\frac{E_r}{M_o\Delta\sigma} \tag{13}$$

The experimental data plotted in figure 5 of the manuscript are coming from acoustic emissions and stick-slip events (McLaskey et al., 2014; Goodfellow and Young, 2014; Yoshimitsu et al., 2014), mining-induced seismicity and excavation undergroung research laboratory (Spottiswoode and McGarr, 1975; Gibowicz et al., 1991; Collins and Young, 2000; Sellers et al., 2003; Oye et al., 2005; Kwiatek et al., 2011), fluid induced seismicity (Urbancic et al., 1993, 1996) and natural earthquakes (Mori et al., 2003; Abercrombie and Rice, 2005; Imanishi and Ellsworth, 2006; Beroza and Spudich, 1988; Baltay et al., 2011; Viesca and Garagash, 2015)

The predictions of the rupture length as a function of the average slip presented in figure **??**b are computed for different values of stress drop following the definition of the average stress drop (Eshelby, 1957)

$$\Delta\sigma = \frac{7\pi}{16}\mu\frac{\bar{D}}{r} \tag{14}$$

for a penny shaped crack of radius r propagating in a homogeneous isotropic infinite medium.

References

Abercrombie, R.E., Rice, J.R.. Can observations of earthquake scaling constrain slip weakening? Geophysical Journal International 2005;162(2):406–424. doi:10.1111/j.1365-246X.2005.02579.x.

Aki, K.. Generation and propagation of g waves from the niigata earthquake of june 16, 1964.: Part 2. estimation of earthquake moment, released energy, and

stress-strain drop from the g wave spectrum. = Bulletin of the Earthquake Research Institute, University of Tokyo 1966;44(1):73–88.

Baltay, A., Ide, S., Prieto, G., Beroza, G.. Variability in earthquake stress drop and apparent stress. Geophysical Research Letters 2011;38(6).

Beeler, N.M., Hickman, S.H.. Stress-induced, time-dependent fracture closure at hydrothermal conditions. Journal of Geophysical Research: Solid Earth 2004;109(B2):1–16. doi:10.1029/2002jb001782.

Beroza, G.C., Spudich, P.. Linearized inversion for fault rupture behavior: Application to the 1984 morgan hill, california, earthquake. Journal of Geophysical Research: Solid Earth 1988;93(B6):6275–6296.

Collins, D.S., Young, R.P.. Lithological controls on seismicity in granitic rocks. Bulletin of the Seismological Society of America 2000;90(3):709–723.

Eshelby, J.D.. The determination of the elastic field of an ellipsoidal inclusion, and related problems. Proceedings of the royal society of London Series A Mathematical and physical sciences 1957;241(1226):376–396.

Freund, L.B.. Dynamic fracture mechanics. Cambridge university press, 1998.

Gibowicz, S., Young, R., Talebi, S., Rawlence, D.. Source parameters of seismic events at the underground research laboratory in manitoba, canada: Scaling relations for events with moment magnitude smaller than- 2. Bulletin of the seismological Society of America 1991;81(4):1157–1182.

Goodfellow, S., Young, R.. A laboratory acoustic emission experiment under in situ conditions. Geophysical Research Letters 2014;41(10):3422–3430.

Imanishi, K., Ellsworth, W.L.. Source scaling relationships of microearthquakes at parkfield, ca, determined using the safod pilot hole seismic array. Earthquakes: Radiated Energy and the Physics of Faulting 2006;170:81–90.

Kammer, D.S., McLaskey, G.C.. Fracture energy estimates from large-scale laboratory earthquakes. Earth and Planetary Science Letters 2019;511:36–43.

Kwiatek, G., Plenkers, K., Dresen, G., Group, J.R.. Source parameters of picoseismicity recorded at mponeng deep gold mine, south africa: Implications for scaling relations. Bulletin of the Seismological Society of America 2011;101(6):2592–2608.

McLaskey, G.C., Kilgore, B.D., Lockner, D.A., Beeler, N.M.. Laboratory generated m-6 earthquakes. Pure and Applied Geophysics 2014;171(10):2601–2615.

Mori, J., Abercrombie, R.E., Kanamori, H.. Stress drops and radiated energies of aftershocks of the 1994 northridge, california, earthquake. Journal of Geophysical Research: Solid Earth 2003;108(B11).

Morrissey, J.W., Geubelle, P.H.. A numerical scheme for mode iii dynamic fracture problems 1997;40(February 1996):1181–1196.

Oye, V., Bungum, H., Roth, M.. Source parameters and scaling relations for mining-related seismicity within the pyhasalmi ore mine, finland. Bulletin of the Seismological Society of America 2005;95(3):1011–1026.

Poliakov, A.N.B., Dmowska, R., Rice, J.R.. Dynamic shear rupture interactions with fault bends and off-axis secondary faulting. Journal of Geophysical Research: Solid Earth 2002;107(B11):ESE 6–1–ESE 6–18. doi:10.1029/2001jb000572.

Sellers, E.J., Kataka, M.O., Linzer, L.M.. Source parameters of acoustic emission events and scaling with mining-induced seismicity. Journal of Geophysical Research: Solid Earth 2003;108(B9).

Spottiswoode, S., McGarr, A.. Source parameters of tremors in a deep-level gold mine. Bulletin of the Seismological society of America 1975;65(1):93–112.

Svetlizky, I., Fineberg, J.. Classical shear cracks drive the onset of dry frictional motion. Nature 2014;509(7499):205–208. URL: http://dx.doi.org/10.1038/nature13202. doi:10.1038/nature13202.

Urbancic, T., Trifu, C.I., Mercer, R., Feustel, A., Alexander, J.. Automatic time-domain calculation of source parameters for the analysis of induced seismicity. Bulletin of the Seismological Society of America 1996;86(5):1627–1633.

Urbancic, T.I., Trifu, C.I., Young, R.P.. Microseismicity derived fault-planes and their relationship to focal mechanism, stress inversion, and geologic data. Geophysical Research Letters 1993;20(22):2475–2478.

Viesca, R.C., Garagash, D.I.. Ubiquitous weakening of faults due to thermal pressurization. Nature Geoscience 2015;8(11):875–879. doi:10.1038/ngeo2554.

Yoshimitsu, N., Kawakata, H., Takahashi, N.. Magnitude- 7 level earthquakes: A new lower limit of self-similarity in seismic scaling relationships. Geophysical Research Letters 2014;41(13):4495–4502.